

Multi-Objective Optimization for Sizing and Control of Microgrid Energy Storage

Kevin Moy

Dept. of Energy Resources Engineering

Stanford University

Stanford, California, USA

kmoy14 [at] stanford.edu

Abstract—Microgrids, electrical power systems that are able to isolate (island) from the larger electric grid and self-sustain for extended periods of time, provide reliable electricity in the face of an unstable electric grid, increasingly driven by the effects of anthropogenic climate change. Lithium-ion battery energy storage systems (ESS) currently are the dominant energy storage system for electric grid usage, and therefore are used in microgrids as well. For microgrids, ESS are a lifeline during islanding periods when stable grid power is not available, yet lithium-ion ESSs degrade with usage and time. Key to addressing this problem is determining the sizing and control of the microgrid ESS in order to sustain the consumer load demand during islanding periods. This paper presents a multi-objective optimization to address this problem, including a cost function penalty that ensures operation of the ESS that avoids degradation-inducing behaviour. This optimization is implemented in Gurobi and solved for several cases, demonstrating the flexibility of optimization framework as well as the effectiveness of the degradation penalty.

Index Terms—microgrid, optimization, energy storage

I. INTRODUCTION

As the impacts of anthropogenic climate change increase, so do the frequency and intensity of severe weather events, including hurricanes, extreme heat waves, flooding, and the increased risk for wildfires [1], [2]. In California, nine of the twenty largest wildfires and five of the twenty deadliest wildfires have occurred in the past few years (2017 - 2020) alone [3], [4]. The interplay between wildfires and the electrical grid is complicated: Wildfires threaten electrical infrastructure, leading to power instabilities; on the other hand, improperly maintained electrical equipment can lead to the start of wildfires, as was the case for the deadly Camp wildfire in 2018 [5]. These wildfires and other extreme weather events represent a loss of electrical power for entire communities. Many of these communities are located farther away from city centers and closer to nature, meaning that a) they are most adversely affected by the extreme weather events, and b) they require extended grid infrastructure to reach them, increasing the risk for general power instability and increasing the time needed to repair infrastructure after the event has passed.

Microgrids are a promising solution to the severe weather/power instability problem. The U.S. Department of Energy's Microgrid Exchange Group defines microgrids as, "a group of interconnected loads and distributed energy resources within clearly defined electrical boundaries that acts as a

single controllable entity with respect to the grid. A microgrid can connect and disconnect from the grid to enable it to operate in both grid-connected or island-mode" [6]. Note that this definition of microgrids includes a great deal of flexibility. The load could be a single household, an apartment building, or an entire community such as a university campus, which may be disaggregated into several load components. The generating resources typically include any combination of diesel generators (DG), solar photovoltaics (PV), energy storage systems (ESS), wind turbines, and other resources. Furthermore, the microgrid can be completely off-grid, where the microgrid is permanently electrically isolated from the rest of the electrical grid, external to the microgrid), or grid-tied, where the microgrid is normally connected to the greater grid.

The prevailing technology for microgrid ESS are lithium-ion batteries, which exhibit degradation and the loss of usable capacity with usage. There have been numerous studies that address the issue of degradation of microgrid energy storage as a multi-objective optimization problem. Broadly, this optimization seeks to develop the optimal dispatch (control) and sizing (kW/kWh) of ESS. This balances operating profit, upfront cost (which scales with size), and degradation of the ESS, which is a function of its usage. A multitude of techniques have been applied to this problem, including evolutionary models [7], the discrete Fourier transform [8], and mixed-integer linear programming [9], [10]. Both [11] and [12] use a mixed-integer linear program that simultaneously determines the optimal dispatch as well as the optimal microgrid ESS capacity.

This paper intends to address a simplified version of this problem, by solving for the optimal size and control of an ESS for a microgrid in islanded mode, using the Blue Lake Rancheria microgrid¹ in Northern California as a starting point case study. By forming a multi-objective optimization that considers diesel generator fuel consumption, the size of the ESS, and a simple degradation penalty, this paper demonstrates 1) the applicability of optimization to this problem, and 2) the effects of including degradation-based penalties on the sizing and control of microgrid ESS.

¹<https://schatzcenter.org/blrmicrogrid/>

II. METHODOLOGY

A. System Description

In this paper, a microgrid will be defined in terms of a single aggregate load representing residential loads as well as commercial building loads, with generating resources of a solar PV array, diesel generator, and an ESS, as is the case in the Blue Lake Rancheria microgrid. These components are electrically connected together via a load bus. The microgrid is assumed to be in islanded mode and therefore the load demand must be supplied solely by the diesel generator, solar PV, and ESS. A simplified diagram of this microgrid is shown in Figure 1, showing all possible power flows between components in islanded mode.

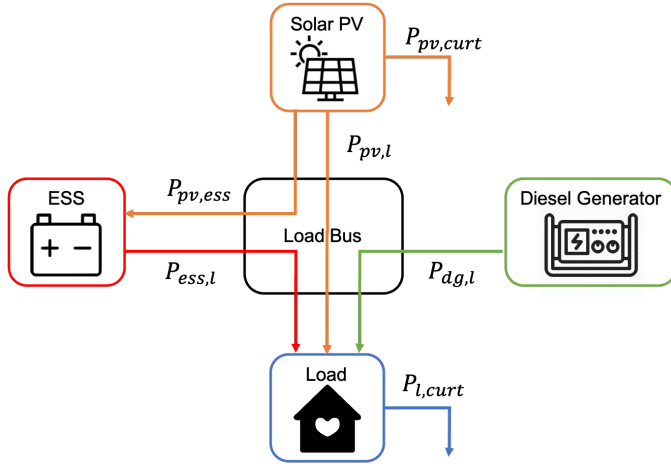


Fig. 1. Power flows in the microgrid, with power flows labelled as defined in Table I. Colors indicate the source of each power flow.

Relevant variables are defined in Table I. The power flows are represented in as time-series data in units of kW, in 15-minute intervals ($h = 0.25$). The curtailed PV power $P_{pv,curt}(t)$ and load power $P_{l,curt}(t)$ are slack variables representing real-life operations: shunting PV output to ground and reducing load consumption in order to balance the supply and demand of power within the microgrid. For the ESS, a fixed duration H is assumed which relates the maximum power output P_{nom} to the maximum energy stored E_{nom} ; that is, an ESS starting fully charged at maximum energy stored E_{nom} can discharge at P_{nom} for H hours.

The islanding period is set to be one week (7 24-hour days), though multiple periods within the year can be considered.

B. Data description

The data used in this paper comes from several sources. First, the Pecan Street database² was used to obtain residential load data. For commercial loads, hospital and school load data were obtained from the DOE Commercial Reference Building Model datasets³ for the San Francisco weather set, which

²<https://www.pecanstreet.org/dataport/>

³<https://openei.org/doe-opendata/dataset/commercial-and-residential-hourly-load-profiles-for-all-tmy3-locations-in-the-united-states>

TABLE I
LIST OF DEFINED VARIABLES IN THE PROBLEM DESCRIPTION.

Variable	Name	Units
h	Period of the data in fractions of an hour	unitless
H	Duration of the ESS	hours
T_w	Number of 15-minute periods in one week	unitless
$l(t)$	Load, total, at time t	kW
$pv(t)$	PV generation, total, at time t	kW
P_{nom}	Maximum power output of the ESS	kW
E_{nom}	Maximum energy stored in the ESS	kWh
$E(t)$	Energy stored in the ESS at time t	kWh
$P_{pv,ess}(t)$	Power flowing from PV to ESS at time t	kW
$P_{pv,l}(t)$	Power flowing from PV to load at time t	kW
$P_{pv,curt}(t)$	PV power curtailed at time t	kW
$P_{ess,l}(t)$	Power flowing from ESS to load at time t	kW
$P_{dg,l}(t)$	Power flowing from DG to load at time t	kW
$P_{l,curt}(t)$	Load power curtailed at time t	kW
$P_{ess,d}(t)$	Power discharged by the ESS at time t	kW
$P_{ess,c}(t)$	Power charged to the ESS at time t	kW
α	Fuel consumption coefficient	L/kWh
η_d	Discharging efficiency of the ESS	unitless
η_c	Charging efficiency of the ESS	unitless
β	Penalty coefficient for charge/discharge	unitless

most closely approximates the weather at the microgrid site. Similarly, the National Solar Resource Database (NSRDB)⁴ was used to obtain solar insolation data near the Blue Lake Rancheria site. Finally, the diesel generator fuel consumption rate of $\alpha = 0.246$ liters per kWh was obtained from [13]. The following paragraphs briefly describe the data processing required for further analysis.

As Pecan Street consists of data from residential homes in various locations, several homes in the Berkeley and Oakland area were selected to form the residential data, as these homes were geographically closest to the Blue Lake Rancheria in the Pecan Street database. In total, 18 homes were found in these locations with complete 15-minute load data, and this load was aggregated and multiplied by a factor of 10 to represent 180 residential homes.

The commercial building loads from the DOE dataset are represented as 1-hour load data, scaled to a peak load of 1000kW. These were then resampled to 15-minute data and scaled down 25% (i.e. to a peak load of 250kW) to reflect the actual peak loads of the Blue Lake Rancheria microgrid. Combined with the aggregate residential load, this forms the aggregate microgrid load, l .

The NSRDB solar insolation data is normalized to 1. Therefore, to obtain the solar PV generation data, this was simply upscaled to 660 kW to represent the power output pv of the solar PV array at Blue Lake Rancheria.

C. Optimization problem

The optimal microgrid has four objectives: minimize emissions, deliver reliable power, minimize cost, and reduce degradation of the ESS. The resulting multi-objective cost function is taken over the week of islanded operation (from $t = 0$ to $t = T_m$), and the optimization can be summarized as

⁴<https://nsrdb.nrel.gov/>

$$\begin{aligned} \text{minimize } & \left[\sum_{t=0}^{T_m} \alpha h P_{dg,l}(t) + \sum_{t=0}^{T_m} P_{l,curt}(t) \right. \\ & \left. + P_{nom} + J_{deg} \right] \end{aligned} \quad (1)$$

The four terms of the cost function are the fuel consumption, curtailed load, power size of the ESS (which scales with cost), and a degradation penalty, respectively corresponding to the four optimal microgrid objectives. P_{nom} is restricted to be between 200kW and 2MW (i.e. $P_{nom} \in [200, 2000]$), reflecting realistic sizes for microgrid ESS. The degradation penalty is a simple quadratic penalty on the charging and discharging power

$$J_{deg} = \beta \sum_{t=0}^{T_m} [P_{ess,c}(t)^2 + P_{ess,d}(t)^2] \quad (2)$$

As high power charge/discharge of the battery could lead to higher degradation. A similar penalty was taken in [14]. The scaling constant $\beta = 0.00005$ was chosen so that the degradation penalty did not saturate the cost function (which would drive charge and discharge power to 0).

The constraints are as follows. First, the power flow in the system at all times t must be respected

$$pv(t) = P_{pv,ess}(t) + P_{pv,l}(t) + P_{pv,curt}(t) \quad (3)$$

$$l(t) = P_{pv,l}(t) + P_{ess,l}(t) + P_{dg,l}(t) + P_{l,curt}(t) \quad (4)$$

$$P_{ess,c}(t) = P_{pv,ess}(t) \quad (5)$$

$$P_{ess,d}(t) = P_{ess,l}(t) \quad (6)$$

Notably, the ESS is restricted to only charge off of solar PV, and can only discharge to the load. The former is a design choice reflecting the objective to reduce fuel emissions, while the latter is a physical constraint (as moving power to either the PV or DG could damage the equipment).

Next, the power and energy constraints of the ESS must be respected, for all times t

$$0 \leq P_{ess,c}(t) \leq P_{nom} \quad (7)$$

$$0 \leq P_{ess,d}(t) \leq P_{nom} \quad (8)$$

$$0 \leq E(t) \leq E_{nom} \quad (9)$$

$$(10)$$

The power-energy ratio H must also be included, to scale E_{nom} with P_{nom} during the optimization

$$E_{nom} = H P_{nom} \quad (11)$$

Next, the time-evolution of energy stored must also be considered. The ESS is assumed to start the islanding period with half of the maximum stored energy, and from then ($t > 0$) changes with the charging and discharging of the ESS

$$E(0) = 0.5 E_{nom} \quad (12)$$

$$E(t) = E(t-1) + h [\eta_c P_{ess,c} - \eta_d P_{ess,d}], \quad t > 0 \quad (13)$$

Where charging increases the energy in the ESS, and discharging decreases it, scaled by the charging and discharging efficiencies.

Finally, the physical properties of the ESS must be considered. The ESS cannot charge and discharge at the same time. Optimizations that allow for such behavior, and do not constrain against such behavior, have been proven to be sub-optimal [15]. This paper follows one approach presented in [15], which introduces a non-convex constraint applied for all times t

$$P_{ess,c} P_{ess,d} = 0 \quad (14)$$

This ensures that at least one of $P_{ess,c}$ or $P_{ess,d}$ is zero, and therefore that they cannot both be nonzero. Therefore, convex optimization solvers and platforms such as CVX can no longer be applied. Instead, Gurobi and its Python API extension were used to construct and solve the optimization [16]. Code can be found at the author's GitHub.⁵

III. RESULTS

The optimization results are presented below for four test cases:

- 1) a 4-hour duration ESS (i.e. $H = 4$) in the first week of the year without the degradation penalty;
- 2) a 4-hour duration ESS in the first week of the year with degradation penalty,
- 3) an 8-hour duration (i.e. $H = 8$) ESS in the first week of the year without the degradation penalty; and
- 4) a 4-hour duration ESS in the 30th week of the year without the degradation penalty.

The results of each optimization case are summarized in Table II, and described in detail in the following subsections.

TABLE II
SUMMARY OF RESULTS

Case	Fuel Consumption [L]	Load Curtailed [kWh]	ESS Power [kW]
1	4701	0	248
2	4714	0	240
3	2758	0	2000
4	8605	0	322

A. $H = 4$, Week 1, No Degradation

Figure 2 shows the result of the optimization in terms of the power flow in the microgrid over the week-long islanding period, while Figure 3 shows the ESS stored energy throughout the same period. The ESS charges off of the excess PV generation, and supplies power to the load when possible. Notably, the ESS spends most of its active charge/discharge

⁵<https://github.com/kmoy14-stanford/AA222FinalProject>

at the maximum rated power (200kW) as determined by the optimization, which could have detrimental degradation effects on the ESS. The DG fills in the load supply that is not met by either PV or ESS and would otherwise be curtailed, leading to no load curtailment over the islanding period.

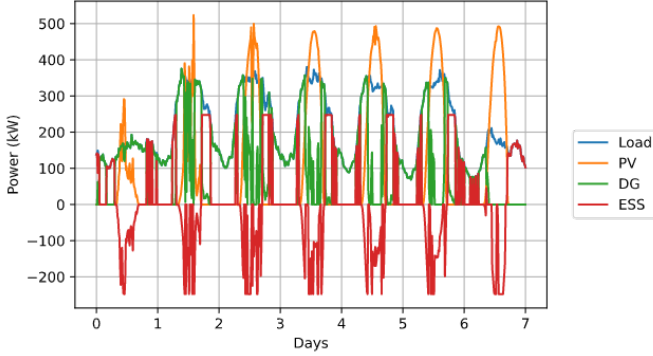


Fig. 2. Power generation and consumption in the microgrid for $H = 4$ in the first week of the year, without degradation penalty. ESS discharge is positive, while ESS charge is negative.

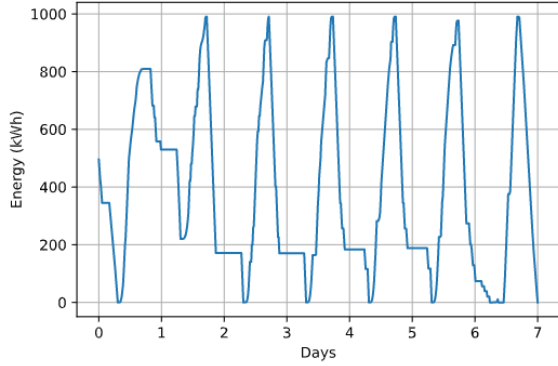


Fig. 3. ESS stored energy for $H = 4$ in the first week of the year, without degradation penalty.

B. $H = 4$, Week 1, Degradation

With the degradation penalty, the results as displayed in Table II are similar to those without the degradation penalty. However, the differences can clearly be seen in the power flow in the microgrid presented in Figure 4. The charging and discharging power is restricted to well below the ESS maximum power of 200kW determined by the optimization. However, the fuel consumption remains the same. This means that the optimization with the degradation penalty produced a control strategy that could lead to lower degradation of the ESS, with minimal gain in fuel consumption and no gain in load curtailment. As a bonus, the average ESS stored energy shown in Figure 5 is lower than that of the case without a degradation penalty in Figure 3, which can also help avoid degradation.

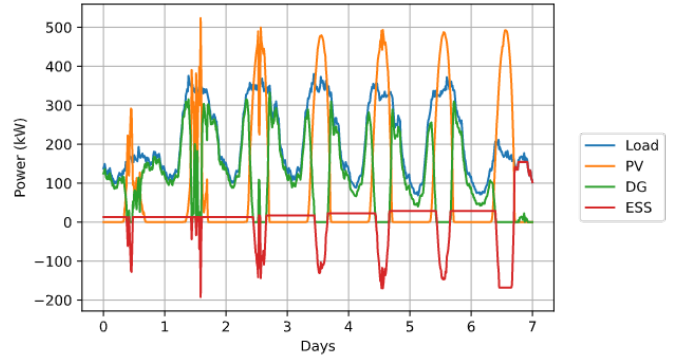


Fig. 4. Power generation and consumption in the microgrid for $H = 4$ in the first week of the year, with degradation penalty. ESS discharge is positive, while ESS charge is negative.

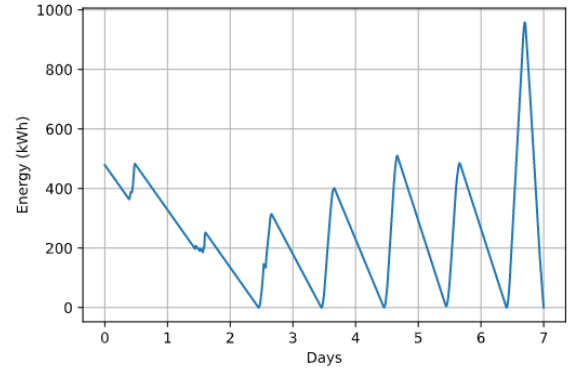


Fig. 5. ESS stored energy for $H = 4$ in the first week of the year, with degradation penalty.

C. $H = 8$, Week 1, No Degradation

Now, the impacts of increasing ESS duration H will be demonstrated, by increasing H from 4 hours to 8 hours. From Table II, with $H = 8$ the fuel consumption is decreased compared to $H = 4$, while the ESS power is set to the maximum 2000kW. The effects of this can be seen in the power flow in the microgrid presented in Figure 6. The ESS is able to supply the majority of the load demand when the PV is not producing power (i.e. at night), and the DG is used only sparingly during the day, in stark contrast to the first two cases. The ESS power is maximized in this case possibly to provide the maximum stored energy. This can be seen in Figure 7, which shows the stored energy decreasing over time. This is in contrast to the previous two cases, which showed the stored energy cycling during each day, largely returning to the same stored energy at the beginning of each day.

D. $H = 4$, Week 30, No Degradation

In this case, the time of the year is different: Week 1 is the first week of the year (winter in the Northern Hemisphere), while Week 30 is in late July/early August (late summer), which is typically the hottest time of the year in Northern California. Thus, the load is higher in Week 30 than in Week 1, and in the case of this dataset, load exceeds PV generation for

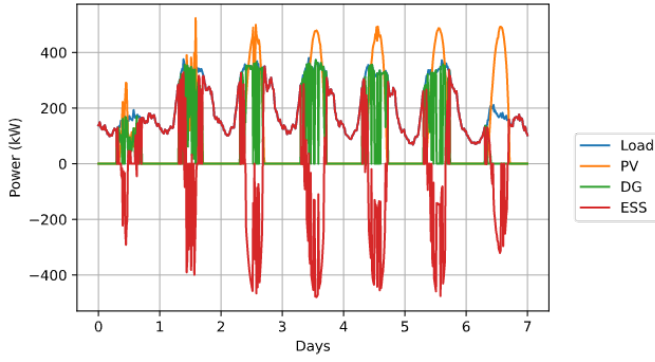


Fig. 6. Power generation and consumption in the microgrid for $H = 8$ in the first week of the year, without degradation penalty. ESS discharge is positive, while ESS charge is negative.

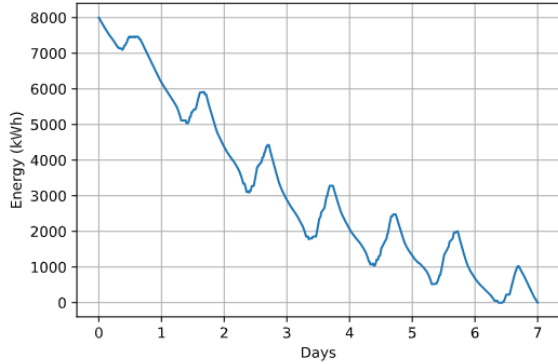


Fig. 7. ESS stored energy for $H = 8$ in the first week of the year, without degradation penalty.

most of the week. The results in Table II reflect this scenario: DG fuel consumption is increased to meet the higher demand, as is the ESS size. The resulting power flow and ESS stored energy are shown in Figure 8 and Figure 9, respectively.

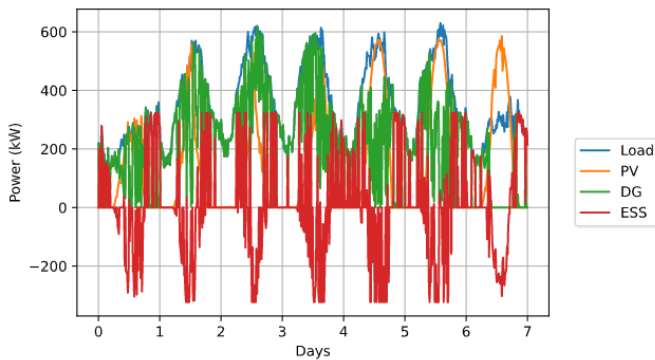


Fig. 8. Power generation and consumption in the microgrid for $H = 4$ in the 30th week of the year, without degradation penalty. ESS discharge is positive, while ESS charge is negative.

IV. CONCLUSION

A multi-objective framework for optimizing the sizing and control of microgrid ESS in islanded mode was presented

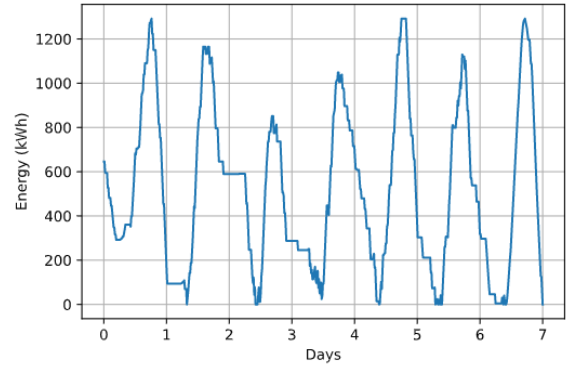


Fig. 9. ESS stored energy for $H = 4$ in the 30th week of the year, without degradation penalty.

and implemented in Gurobi. Several different cases were presented using a microgrid modelled after the Blue Lake Rancheria microgrid, showing the flexibility and adaptability of the optimization to consider different microgrid islanding scenarios. Furthermore, a degradation penalty was shown to significantly alter the ESS charging and discharging behavior to potentially reduce degradation of the ESS, with little to no effect on fuel consumption and load curtailment.

Future work could consider adding in a more complex model for ESS that accurately models and considers the effect of degradation, and can either act as more-informed degradation penalties or as tighter, time-dependent constraints on the stored energy in the ESS (reducing the stored energy over time as the ESS degrades). The variability of load and PV resource throughout the year could also be taken into account via an optimization that takes into account multiple different islanding periods at once, to arrive at a more generalized optimal size for the ESS. Finally, different multi-objective optimization approaches can be taken to this problem, such as a lexicographic optimization, instead of combining them in a linear fashion as presented in this paper.

ACKNOWLEDGMENT

The author would like to thank the AA 222 course teaching staff for the opportunity to pursue and present this work.

REFERENCES

- [1] A. Williams, J. Abatzoglou, A. Gershunov, J. Guzman-Morales, D. Bishop, J. K. Balch, and D. P. Lettenmaier. Observed Impacts of Anthropogenic Climate Change on Wildfire in California. *Earth's Future*, 7(8):892–910, 08 2019.
- [2] M. Goss, D. Swain, J. Abatzoglou, A. Sarhadi, C. Kolden, A. Williams, and N. Diffenbaugh. Climate change is increasing the likelihood of extreme autumn wildfire conditions across California. *Environmental Research Letters*, 15(9), Aug 2020.
- [3] CAL FIRE. Top 20 largest California wildfires. Technical report, CAL FIRE, 2020.
- [4] CAL FIRE. Top 20 deadliest california wildfires. Technical report, CAL FIRE, 2020.
- [5] Ivan Penn and Peter Eavis. PG&E Pleads Guilty to 84 Counts of Manslaughter in Camp Fire Case. *New York Times*, Jun 2020.
- [6] Office of Electricity Delivery and Energy Reliability Smart Grid R&D Program. DOE Microgrid Workshop Report. United States Department of Energy, 2011.

- [7] S. Singh, M. Singh, and S. C. Kaushik. Feasibility study of an islanded microgrid in rural area consisting of PV, wind, biomass and battery energy storage system. *Energy Conversion and Management*, 128:178 – 190, 2016.
- [8] J. Xiao, L. Bai, F. Li, H. Liang, and C. Wang. Sizing of Energy Storage and Diesel Generators in an Isolated Microgrid Using Discrete Fourier Transform (DFT). *IEEE Transactions on Sustainable Energy*, 5(3):907–916, 2014.
- [9] Y. Wang, Z. Yi, D. Shi, Z. Yu, B. Huang, and Z. Wang. Optimal distributed energy resources sizing for commercial building hybrid microgrids. In 2018 IEEE Power Energy Society General Meeting (PESGM), pages 1–5, 2018.
- [10] V. Francois-Lavet, Q. Gemine, D. Ernst, and R. Fonteneau. Towards the Minimization of the Levelized Energy Costs of Microgrids Using both Long-Term and Short-Term Storage Devices. *Smart Grid: Networking, Data Management, and Business Models*, 217:295–319, 2016.
- [11] H. Xie, X. Teng, Y. Xu, and Y. Wang. Optimal energy storage sizing for networked microgrids considering reliability and resilience. *IEEE Access*, 7:86336–86348, 2019.
- [12] I. Alsaidan, A. Khodaei, and W. Gao. A Comprehensive Battery Energy Storage Optimal Sizing Model for Microgrid Applications. *IEEE Transactions on Power Systems*, 33(4):3968–3980, 2018.
- [13] M. Alramlawi, A. Femi Timothy, A. Gabash, E. Mohagheghi and P. Li, Optimal Operation of PV-Diesel MicroGrid with Multiple Diesel Generators Under Grid Blackouts. 2018 IEEE International Conference on Environment and Electrical Engineering and 2018 IEEE Industrial and Commercial Power Systems Europe, pp. 1-6, 2018.
- [14] F. Aghdam, N. Kalantari, B. Mohammadi-Ivatloo, A Chance-Constrained Energy Management in Multi-Microgrid Systems Considering Degradation Cost of Energy Storage Elements. *Journal of Energy Storage*, Volume 29, 101416, 2020.
- [15] K. Garifi, K. Baker, D. Christensen, B. Touri. Control of Energy Storage in Home Energy Management Systems: Non-Simultaneous Charging and Discharging Guarantees. *arXiv:1805.00100*, 2018.
- [16] Gurobi Optimization, LLC. Gurobi Optimizer Reference Manual. <http://www.gurobi.com>, 2021.